Phosphorus, sodium and sulphur measurements in compound samples using 2.5 MeV neutron activation

Fatai. A. Liadi[1] · A. A. Naqvi[1] · F. Z. Khiari[1] · M. Raashid[1]

Abstract

Phosphorous, sodium, and sulphur concentrations in soil mixed with sodium triphosphate, magnesium sulphate, and sodium chloride were analyzed in neutron activation with 2.5 MeV neutron dc beams using BGO and $CeBr_3$ detectors. Also, sulphur mixed with soil was analyzed using the BGO detector. The Minimum Detectable Concentrations were in the 0.31 ± 0.09–0.79 ± 0.24 wt.% range. The MDC of sulphur in magnesium sulphate measured by the BGO detector agrees with the previously reported value using the $CeBr_3$ detector. This study has provided useful data on MDCs of phosphorus, sodium, and sulphur in composite/compound bulk samples in fast neutron inelastic scattering.

Keywords Sodium triphosphate (STP), $MgSO_4$ (MgS) and NaCl samples · BGO and $CeBr_3$ detectors · 2.5 MeV neutrons · Portable neutron generator based activation setup · Minimum detectable concentration · Measurements of phosphorus Sodium and sulfur concentrations

Introduction

With advances in nuclear technology, the application of Fast Neutron Activation is rapidly expanding in diverse areas; such as health sciences, nuclear engineering, environmental sciences, mining industries and biosciences [1–3]. Major advances have been made in the development of portable 14 and 2.5 MeV neutron generators with higher fast neutron fluxes. Typical examples are high flux neutron generators from Sodern model Genie 35 and Adelphi technology model DT110 for14 MeV neutrons [2]. Recently, a new D-D neutron generator has been developed in collaboration with Adelphi Technology for prompt gamma activation analysis [3]. Prompt gammas can be excited in the nucleus via thermal neutron capture and fast neutron inelastic scattering [3, 4]. Particularly, 3 and 14 MeV neutron beams from DD and DT neutron generators have been used successfully in prompt gamma elemental analysis in fast neutron inelastic studies [1–4]. Some of the elements have been analyzed with 3 MeV neutron beams via (n, γ), (n, p) and (n, n'γ) fast neutron reactions [5–9]. Recently, Naqvi et al. [7] have used

2.5 MeV fast neutron beams from a DD neutron generator to carry out elemental analysis of sulfur in bulk samples.

Nuclear detection and measurement of elemental concentrations of elements of interest in soil can be done using passive methods for radioactive elements using gamma-ray spectrometry, as reported in the recent work of Kavetsky et al. [13]. On the other hand, elemental analysis of other elements (not naturally radioactive) in soil samples can be achieved using neutron activation analysis. This nuclear technique complements those based on chemical or other physical methods and enjoys some advantages when compared to them. These can be summarized in the bulk nature of the samples, the simple and limited nature of sample preparation, as well as the nondestructive nature of the analysis. This is due to the highly penetrating power of the neutrons as well as the gamma rays resulting from neutron activation. This results in the possibility of analyzing large samples with the whole sample volume being interrogated [14]. These properties make neutron activation analysis very versatile and suited for the analysis of a large variety of bulk solid and liquid samples. As very recent pertinent examples of analysis of bulk solids, we mention the work of Hei et al. [15] using a neutron inelastic scattering system based on a DT neutron generator for the analysis of metallic materials, and the work of Abel and Nie [16] for improving the fast

✉ F. Z. Khiari
  Khiari@kfupm.edu.sa

1 Department of Physics, King Fahd University of Petroleum and Minerals, Dhahran, Saudi Arabia

neutron inelastic scatter analysis to iron using the associated particle collimation method.

In a continuation of the previous study [7], more complex compound bulk samples have been analyzed using neutron inelastic studies utilizing 2.5 MeV neutron beams from a DD neutron generator. In this regard, phosphorus and sodium concentrations have been determined in STP. MgS, NaCl and S-Soil bulk samples. In the following the present study along with the results are described.

Experimental

In this study, samples were analyzed to measure Phosphorus, Sodium and Sulfur concentrations in compound STP, MgS, NaCl and S-soil (Sulphur-in-soil) samples using a BGO and a $CeBr_3$ detectors. The STP, MgS, NaCl, and S-soil were prepared by thoroughly mixing the respective elements with soil. The samples were then filled in cylindrical plastic bottles with 90 mm × 140 mm (diameter x height) dimensions. The mass of each empty bottle was 58.0 g. The bottles are made up of PET polymer chain with the chemical formula $(C_{10}H_8O_4)_n$. The total mass of the each sample was fixed at about 1610 g. Table 1 shows the elemental concentrations in the samples.

The analyses were carried out after irradiation of empty and filled sample containers with dc beams of 2.5 MeV neutrons produced by 70 keV deuterons with 50 µA beam current. The 2.5 MeV neutrons were produced in the exoergic $D(d,n)^3He$ reaction and their intensity from the Genie 16 neutron generator was around 4.7×10^7 n/s. This intensity was recorded by a built in neutron intensity monitor which displays it as calculated from the deuterium beam current of a given energy and deuterium target initial loading. The neutron intensity is quoted for a nominal energy of 2.5 MeV. The mid sample position is around 7 cm away from the target site and, consequently, the fast neutron intensity at the sample position should be slightly less than 4.7×10^7 n/s. During the experiment, we only monitor the variation in neutron flux over the duration of the irradiation. The monitor reading is recorded in order to perform any needed correction due to neutron flux fluctuation [7]. Moreover, the energy spectrum of neutrons produced in the $D(d,n)^3He$ reaction

Table 1 Elemental concentrations in the compound samples

Sample	Element	Element-Conc. (wt.%)
P-STP	P	1.4, 2.8 and 4.49
	Na	3.11, 6.23, and 9.99
MgS	Mg	1.89, 3.01 and 4.0
	S	2.5, 4.0, and 5.3
NaCl	Na	6.23, 9.99, and 12.46
S-soil	S	4.4, 7.1, 9.6 and 13.47

using 0.1 MeV incident deuteron energies has a maximum energy of 2.85 MeV at 0°, a minimum energy of 2.15 MeV at 180°, and 2.5 MeV at 90° [20]. Some details about the Monte Carlo simulation of the transport of neutrons from the target site to the sample position, generation of gamma-rays from inelastic neutron scattering with elements in the sample and their transport to the detector volume can be found in the prequel to this work as reported in [7].

The prompt gamma-ray data from the contaminated soil samples were acquired for pre-set times using a Multi-channel Buffer-based data acquisition system, supplied by EG&G Ortec-USA, coupled to a PC-based workstation. The Multi-channel Buffer utilizes the Scinti Vision software from Ortec for data acquisition and analysis [17]. The data collection times from the samples were 15–60 min. The dead-time of the pc-based data acquisition system was typically less than 1%. For peak identification, the gamma ray spectra were calibrated using a Bi-207 gamma ray calibration source with 570, 1024 and 1772 keV mono energetic gamma rays.

During exposure to 2.5 MeV neutrons, the detectors emit prompt gamma rays due to neutron inelastic scattering and thermal neutron capture in the detector materials. The BGO detector background mainly consists of Bi, Ge and O elements prompt capture gamma rays with peaks at 575, 595, 852, 868, 1204, 1636 and 1641 keV from Ge due to neutron absorption resulting from multiple scattering of 2.5 MeV neutrons in the detector material. Similarly, for the $CeBr_3$ detector, the detector background spectrum shows gamma rays from Ce, Br-79 and Br-81 in the detector material with energies of 219, 275, 542, 569, 648, 824, 846, 972, 1133 keV from bromine and 1347 keV gamma rays from cerium.

Prompt gamma analysis of STP and NaCl samples using BGO and $CeBr_3$ detectors

In this part of the study the gamma ray spectra from STP and NaCl samples were analyzed using 76 mm × 76 mm (diameter x height) BGO as well as $CeBr_3$ detectors. These detectors are manufactured by Scionix Holland company with decay times of 300 ns and 19 ns as well as energy resolutions of 11.0% and 4.0% at 662 keV of Cs-137, respectively. The STP samples contained 1.4, 2.8 and 4.49 wt. % P and 3.11, 6.23 and 9.99 wt.% Na while the NaCl samples contained 6.23, 9.99, and 12.46 wt. % Na (Fig. 1).

A, bshow the gamma ray spectra from STP samples superimposed upon the background spectrum over 0–2.20 and 1.1–2.64 MeV energy range, respectively. The Na peak at 438 keV is quite prominent in Fig. 2a while Fig. 2b shows a prominent peak of P at 2230 keV.

Figure 3a, b show the prompt gamma ray spectra over 0–0.93 and 1.61–2.73 MeV range, respectively, from STP
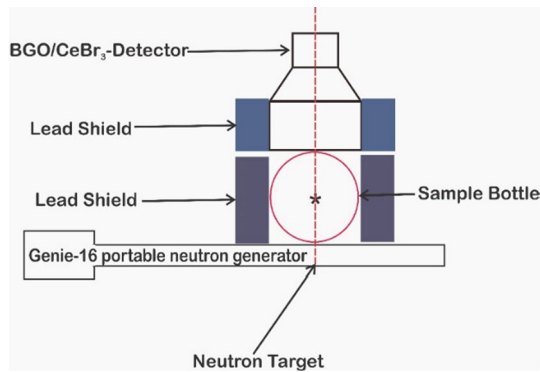
Fig. 1 Schematic diagram of 2.5 MeV Neutron -based PGNAA Setup built around a Genie-16 portable neutron generator
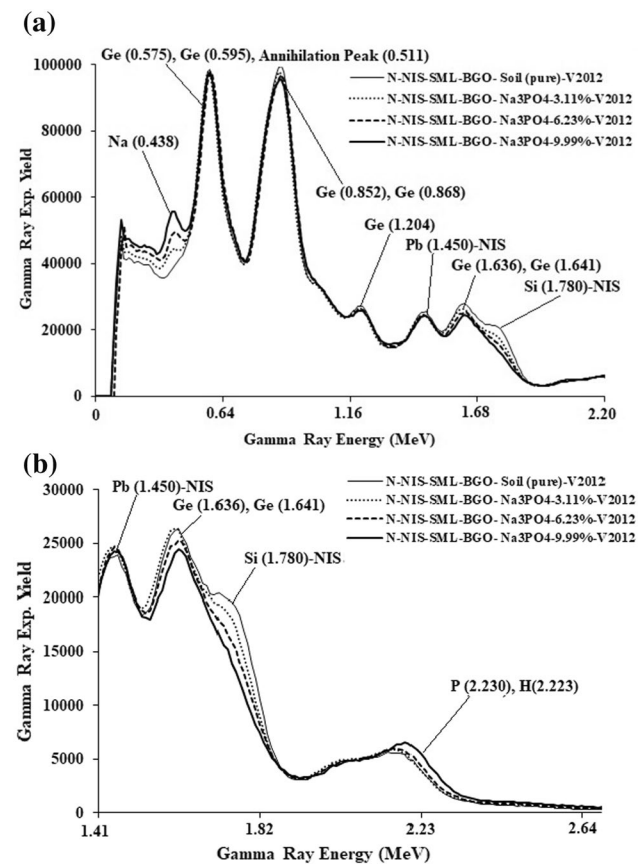

Fig. 2 a Prompt gamma-rays pulse height spectra of STP samples over 0–2.20 MeV containing 3.11, 6.23 and 9.99 wt.% sodium along with background spectrum taken with BGO detector. **b** Prompt gamma-rays pulse height spectra of STP samples over 1.41–2.64 MeV containing 1.4, 2.8 and 4.49 wt.% phosphorus along with background spectrum taken with BGO detector
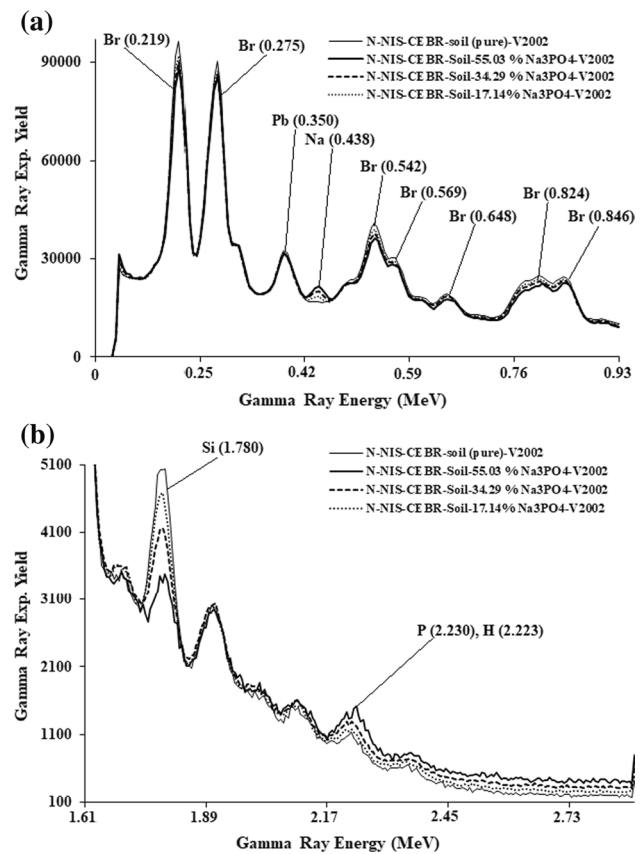

Fig. 3 a Prompt gamma ray spectra of STP samples superimposed upon background spectrum over 0–0.93 MeV energy range taken with CeBr$_3$ detector. **b** Prompt gamma ray spectra of STP samples superimposed upon background spectrum over 1.61–2.84 MeV energy range taken with CeBr$_3$ detector

samples superimposed upon the background spectrum using the CeBr$_3$ detector keeping the same beam parameters as with the BGO detector. The spectra show the 438 keV sodium and 2230 keV phosphorus peaks along with the 1780 keV silicon peak along with the CeBr$_3$ detector background peaks.

Finally, NaCl samples containing 6.23, 9.99, and 12.46 wt.% sodium concentrations mixed with soil were analyzed using the BGO and CeBr$_3$ detectors keeping the same beam parameters as used in the analysis of STP samples. Figure 4a, b show gamma-rays pulse height spectra of NaCl samples containing 6.23, 9.99, and 12.46 wt.% sodium superimposed upon the background spectrum from the BGO detector and the CeBr$_3$ detector, respectively.

The integrated yields of P and Na peaks in STP and NaCl samples were calculated by integrating the counts under each peak with respect to a window of 3–15 channels wide centered around the peak channel location. The integrated yield from each spectrum was normalized to the same neutron flux and data acquisition time using the beam current monitor of the neutron generator. The least square fit of the normalized total net counts as a function of element concentration in wt. % for each peak was then used to obtain the slope (counts/ wt. % element) and the intercept (background counts) for
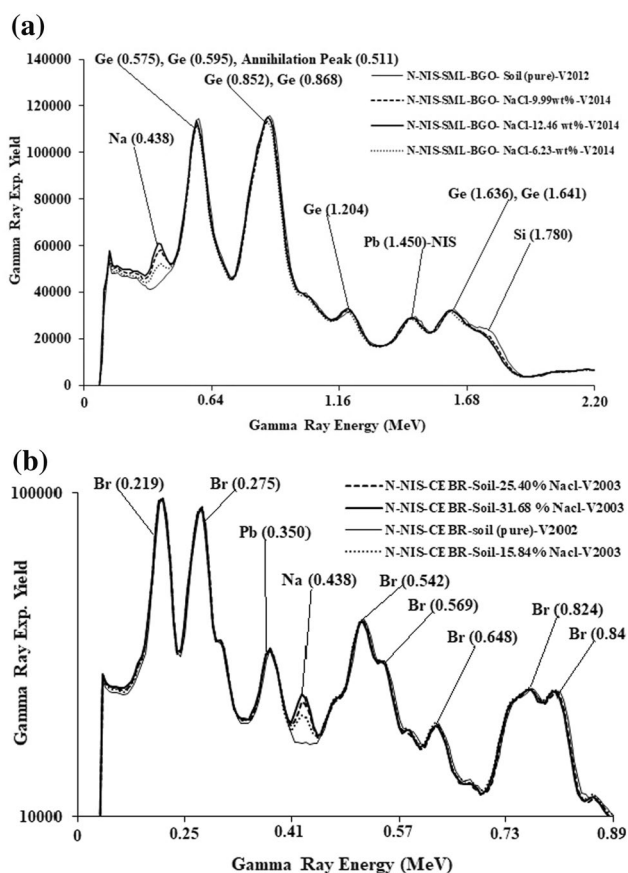
(a)

(b)

Fig. 4 **a** Prompt gamma-rays pulse height spectrum of NaCl sample containing 6.23, 9.99, and 12.46 wt% sodium superimposed upon background spectrum using BGO detector. **b** Prompt pulse height spectra of NaCl samples contain 6.23, 9.99, and 12.46 wt% sodium concentration superimposed upon background spectrum taken with CeBr$_3$ detector

(a)

(b)

Fig. 5 **a** Prompt gamma ray yield as a function of P concentration in STP samples taken with the BGO and CeBr$_3$ detectors. **b** Prompt gamma ray yield as a function of Na concentration in STP and NaCl samples taken with the BGO and the CeBr$_3$ detectors

MDC and σ_{MDC} Eqs. (1) and (2). The slopes of the calibration curves in Fig. 5a, b, as well as Fig. 7, and the statistical uncertainties on them were calculated from the error-weighted averages of the normalized total net counts and the statistical uncertainties on them [18]. The window width was optimized to obtain the optimum value of MDC $\pm \sigma_{MDC}$. Figure 5a shows the prompt gamma ray yield of the P peak as a function of phosphate concentration in STP samples for the BGO and CeBr$_3$ detectors after background subtraction. For the BGO detector, the P concentration curve has a slope of 5586 counts/wt. % P concentration while for the CeBr$_3$ detector the slope of P concentration is 1188 counts/wt. % P concentration, which is clearly smaller than that for the BGO detector.

Figure 5b shows the prompt gamma ray yield of the sodium peak as a function of Na concentration in STP and NaCl samples taken with the BGO and the CeBr$_3$ detectors. For the BGO detector, the slope of Na peak for STP samples is 6429 counts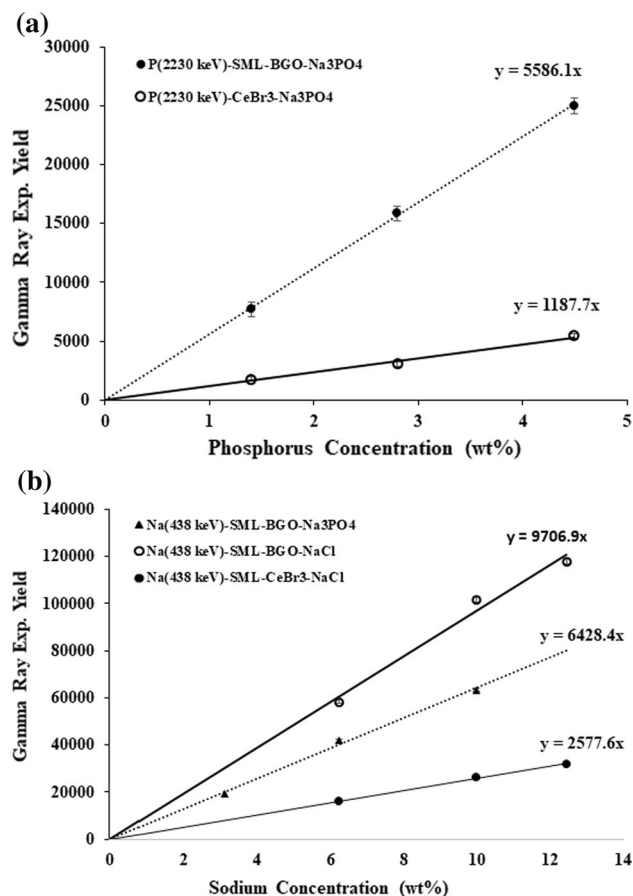/wt. % Na, while for NaCl samples the slope is 9707 counts/wt. % Na. For the CeBr$_3$ detector, the slope for the Na peak is 2578 counts/wt. % Na.

Prompt gamma analysis of MgS and S-soil samples

In the second part of the study, MgS as well as S- soil samples have been analyzed through 2.5 MeV fast neutron activation using the same BGO detector as used for STP samples and the same neutron beam parameters as used with STP and NaCl samples. Prompt Gamma Ray analysis of MgS samples with 1.89, 3.01 and 4.0 wt.% Mg and 2.5, 4.0 and 5.3 wt.% S were analyzed along with S- soil samples containing 4.4, 7.1, 9.6 and 13.47 wt.% of Sulphur. Figure 6a shows the spectrum for a MgS sample containing 5.3 wt.% sulfur over 0—2.88 MeV energy range superimposed upon a soil sample background taken with the BGO detector. The Figure also shows the 1780 keV Si peak along with the 2240 keV S peak as well as the 1450 keV peak due to inelastic scattering from lead
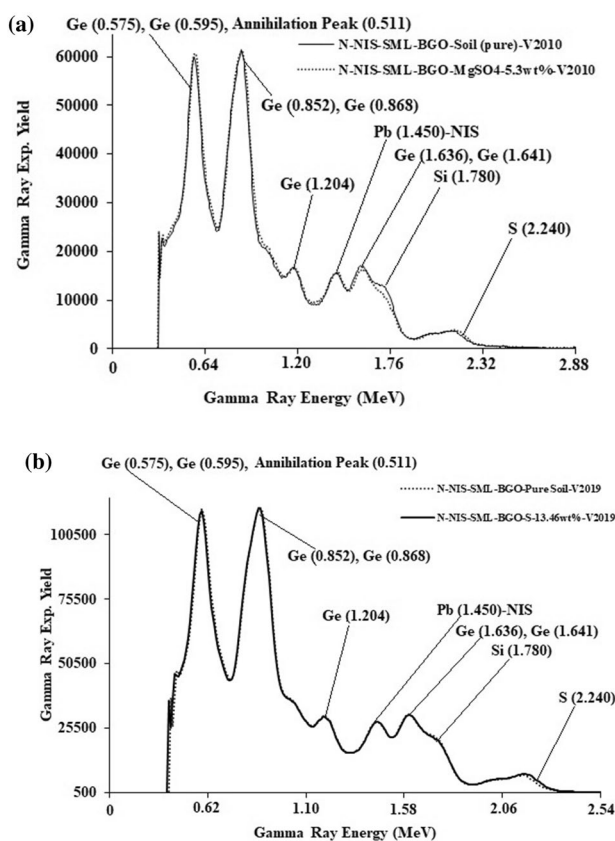
Fig. 6 **a** Prompt gamma rays pulse height spectrum of MgSO4 with 5.3 wt.% S superimposed upon soil background over 0–2.88 MeV taken with the BGO detector. **b** Prompt gamma rays pulse height spectrum of S-soil with 13.46 wt. % S superimposed upon soil background over 0–2.54 MeV taken with the BGO detector
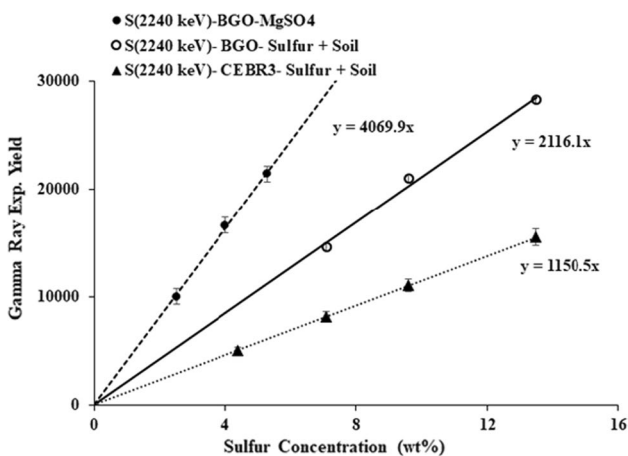

Fig. 7 Sulfur Prompt gamma ray yield as a function of sulfur concentration in MgS and S-soil samples using the BGO detector along with previously published data with a CeBr$_3$ detector for S-soil samples

blocks in the shielding. Due to the low concentration of Mg in the MgS sample, 582 keV gamma rays from Mg could not be detected by the BGO detector and are not visible in Fig. 6a. Therefore, in the remaining part of the study we concentrated only on S detection in the MgS samples. Figure 6b shows the S-soil sample spectrum over 0—2.54 MeV energy range containing 13.46 wt.% S superimposed upon the soil background spectrum.

As in the case of STP and NaCl samples, integrated yields of S peaks in MgS and S-soil samples were calculated by integrating the counts under each peak with respect to a window of 3–15 channels wide centered around the peak channel location for the BGO detector. The integrated yield from each spectrum was normalized to the same neutron flux and data acquisition time using the beam current monitor of the neutron generator. As was done with P and Na, the least square fit of normalized total net counts as a function of element concentration in wt. % for each peak was used to obtain the slope (counts/wt. % element) and the intercept (background counts) for MDC and σ_{MDC} calculations [18]. The window width was optimized to obtain the optimum value of MDC $\pm \sigma_{MDC}$. Figure 7 shows the prompt gamma ray yield of S peak as a function of sulfur concentration in MgS and S-soil samples for the BGO detector after background subtraction. For the MgS samples, the S concentration curve has a slope of 4070 gamma rays per wt. %, while that from S-soil samples is 2116 per wt. %. For the CeBr$_3$ detector, the previously reported slope from S-soil samples is 1150 per wt. %.

MDC calculations of P, Na and S in STP, MgS, NaCl and S-soil samples using the CeBr$_3$ and BGO detectors

The minimum detectable concentrations (MDC) of P, Na and S in STP, NaCl, MgS and S-soil samples were determined for the KFUPM PGNAA setup used in this study. The MDC for a peak with net counts P, element's concentration C (wt.%) and associated background counts B (under the peak) can be approximated using the equation [7, 10]

$$MDC = 4.653 \left(\frac{C}{P} \right) \sqrt{B} \tag{1}$$

where C/P: concentration (wt.%)/counts is the inverse of the slope of the concentration curve, i.e. the calibration constant of the setup for a specific gamma ray peak. The corresponding uncertainty.

σ_{MDC} is given by:

$$\sigma_{MDC} = \left(\frac{C}{P} \right) \sqrt{2B} \tag{2}$$

Table 2 shows the MDC $\pm \sigma_{MDC}$ values for P, Na and S in STP, NaCl, MgS and S-soil samples.

Table 2 MDC $\pm \sigma_{MDC}$ [wt.%] of P, Na, and S in STP, NaCl, MgS and S-soil samples

Sample	Element	Present Study		Naqvi[7]	Jiggins[5]
		MDC $\pm \sigma_{MDC}$			
		BGO	CeBr$_3$		
P-STP	P	0.37 ± 0.11	0.55 ± 0.17		0.87
Na-STP	Na	0.31 ± 0.09	0.79 ± 0.24		
Na-NaCl	Na	0.35 ± 0.11	0.73 ± 0.22		
S-MgSO4	S	0.56 ± 0.17			
S-Soil	S	0.68 ± 0.21		0.68 ± 0.21	

For P determination in compound STP samples, while the MDC value of 0.55 ± 0.17 wt.% for the CeBr$_3$ detector is consistent with the value of 0.87 wt.% quoted, without uncertainties, by ref. [5], the MDC value of 0.37 ± 0.11 wt.% using the BGO detector is probably better than the one of Jiggins and Habbani [5]. One reason might be that their neutron yield is about a factor of two less than ours, and their distance from the neutron target to sample position is 51.5 cm [19] while ours was about 7 cm, resulting in a lower fast neutron flux at the sample position in their case. Another reason might be the smaller size of their samples compared to ours [19]. The MDC $\pm \sigma_{MDC}$ value of P in STP samples for the BGO and CeBr$_3$ detectors could be considered consistent with each other, within their experimental uncertainties. However, due to its higher light output, the BGO detector achieves smaller uncertainties in MDC as compared to the CeBr$_3$ detector.

For Na determination in compound STP and NaCl samples using the CeBr$_3$ detector, the MDC $\pm \sigma_{MDC}$ are 0.79 ± 0.24 wt.% and 0.73 ± 0.22 wt.%, respectively. These two MDC values agree with each other. For the BGO detector, the MDC $\pm \sigma_{MDC}$ of Na in STP and NaCl samples are 0.31 ± 0.09 wt.% and 0.35 ± 0.11 wt.%, respectively. The MDC values for the Na peak from the BGO detector agree with each other, but are measurably smaller and have smaller uncertainties as compared to those from the CeBr$_3$ detector because the BGO detector has a higher light output.

For S determination in compound MgS and S-soil samples, the MDC $\pm \sigma_{MDC}$ for the BGO detector are 0.56 ± 0.17 wt.% and 0.68 ± 0.21 wt.%, respectively, in good agreement with each other. Moreover, the MDC value of 0.68 ± 0.21 wt.% for the BGO detector from this study is in total agreement with the MDC value 0.68 ± 0.21 wt.% reported earlier for the CeBr$_3$ detector [7].

The MDC values for the higher efficiency BGO detectors tend to follow the trend for the inverse of the NIS cross sections for P Na and S, i.e. $\sigma_{NIS-P} = 350$ mb; $\sigma_{NIS-Na} = 321$ mb; $\sigma_{NIS-S} = 175$ mb; [11, 12].

Conclusion

Concentrations of P, Na and S in STP, MgS and NaCl samples were determined in neutron activation with 2.5 MeV dc neutron beams using BGO and CeBr$_3$ detectors. Also, S-soil samples were analyzed for S using the BGO detector. For STP samples, the minimum detectable concentration (MDC $\pm \sigma_{MDC}$) of P has been calculated to be 0.37 ± 0.11 wt.% and 0.55 ± 0.17 wt. % for the BGO and CeBr$_3$ detectors, respectively, whereas the MDC values of Na in STP samples were 0.31 ± 0.09 and 0.79 ± 0.24 wt.% for the BGO and CeBr$_3$ detectors, respectively. For NaCl samples, the MDC values for Na were 0.35 ± 0.11 and 0.73 ± 0.22 wt. % for the BGO and CeBr$_3$ detectors, respectively. The MDC values of S in MgS and S-soil samples were 0.56 ± 0.17 wt. % and 0.68 ± 0.21 wt.%, respectively, using the BGO detector. The MDC value of S in MgS samples measured by a BGO detector is in total agreement with the previously reported MDC value of 0.68 ± 0.21 wt. % for a CeBr$_3$ detector [7]. This study has provided useful data on MDC values of P, Na, and S in composite/compound bulk samples in fast neutron NIS scattering.

References

1. Neutron Generators for analytical Purposes (2012) IAEA radiation technology reports series No. 1, (IAEA radiation technology reports series, ISSN 2225–8833; no. 1) STI/PUB/1535 ISBN 978–92–0–125110–7; International Atomic Energy Agency Vienna

2. Marchese N, Cannuli A, Caccamo MT, Pace C (2017) New generation non-stationary portable neutron generators for biophysical applications of neutron activation analysis. Biochem Biophys Acta 1861(2017):3661–3670

3. Bergaoui K, Reguigui N, Gary CK, Brown C, Cremer JT, Vainionpaa JH, Piestrup MA (2014). Development of a new

deuterium-deuterium generator for prompt gamma-ray neutron activation analysis. Appl Radiation Isotopes 94:319–327

4. Thompson LC (1952) Gamma rays produced by the inelastic scattering of 14 MeV neutrons. The Rice Institute, Houston, Texas

5. Jiggins AH, Habbani FI (1976) Prompt gamma-ray analysis using 3.29 MeV neutron inelastic scattering. Int J Appl Radiat Isot 27:689–693

6. Scherrer VE, Allison BA, Faust WR (1954) Gamma radiation from interaction of 3.2-mev neutrons with various materials. Phys Rev 96(2): 386–388

7. Naqvi AA, Khiari FZ, Al-Abdallah T, Liadi FA, Raashid M, Isab AA (2019) Detection of sulfur in soil samples using 2.5 MeV neutron activation. J Radioanal Nuclear Chem. Doi: https://doi.org/10.1007/s10967-019-06589

8. Cazzaniga C, Nocente M, Tardocchi M, Croci G, Giacomelli L, Angelone M, Pillon M, Villari S, Weller A, Petrizzi L, Gorini G, ASDEX Upgrade Team, JET-EFDA Contributors (2013) Response of LaBr$_3$(Ce) scintillators to 2.5 MeV fusion neutrons. Rev Sci Instrum 84:123505

9. Lind DA, Day RB (1961) Studies of gamma rays from neutron inelastic scattering. Ann Phys 12:485–532

10. Gedcke DA (2001) How counting statistics controls detection limits and peak precision. ORTEC Application Notes AN59. Website: /www.ortec-online. Com

11. Stehn JR, Goldberg MD, Magurno BA, Wener-Chasman R (1964) Neutron cross sections Volume I, Z=1 to 20; Second Edition, Supplement No. 2 (Physics - TID-4500, 32nd Ed.) May I964. Published by Sigma Center Brookhaven National Laboratory Associated Universities, Inc. under contract with the United States Atomic Energy Commission.

12. Garber DI, Kinsey RR (1976) Neutron cross sections, Volume II, Curves-BNL 325 Third Edition, Volume II, (Physics, Nuclear-TID-4500). [EANDC(US)-183], [INDC(USA)-58], Jan, 1976

13. Kavetskiy A, Yakubova G, Sargsyan N, Prior SA, Torbert HA, Chin BA (2021) Measuring and mapping potassium in agricultural fields using gamma spectroscopy. IEEE Trans Nuclear Sci, 68(10). October 2021

14. Alfassi Z (1990) Activation analysis, vol I. CRC Press. ISBN 9780849345838

15. Hei D, Jia W, Cheng C, Yao Z, Shan Q, Ling Y, Lei H (2021) Design of an inelastic neutron scattering system based on DT neutron generator for metallic materials analysis. J Radioanal Nucl Chem 329:301–308

16. Abel MR, Nie LH (2019) Improving the sensitivity of fast neutron inelastic scatter analysis to iron using associated particle collimation. Nuclear Inst Methods Phys Res A 932: 31–42

17. AMETEK America, MAESTRO Multichannel Analyzer Emulation Software. https://www.ortec-online.com/-/media/ametekortec/brochures/maestro.pdf?la=en&revision=081a0cf5-d5a1–441d-b66c-98ff531a7624

18. Bevington PR, Robinson DK (2002) Data reduction and error analysis, 3rd edn, McGraw Hill, New York, pp 98–104 (Chapter 6).

19. Habbani FI, Jiggins AH (1976) Gamma Emission Cross Sections for 23 Elements using 3.29 MeV Neutron Inelastic Scattering. Nuclear Inst. and Methods in Physics Research, 134: 545–552

20. Csikai J (1987) CRC handbook of fast neutron generators. In: Press CRC (ed) Volume I. Florida, Boca Raton, pp 17–18